Lead oxide nanobelts and phase transformation induced by electron beam irradiation

Z. W. Pan, Z. R. Dai, and Z. L. Wang[a)]
School of Materials Science and Engineering, Georgia Institute of Technology, Atlanta, Georgia 30332-0245

(Received 13 August 2001; accepted for publication 30 October 2001)

β-PbO_2 nanobelts, with a rectangular cross section, a typical length of 10–200 μm, a width of 50–300 nm, and a width-to-thickness ratio of 5–10, have been successfully synthesized by simple elevated evaporation of commercial PbO powders at high temperature. The PbO_2 nanobelts are enclosed by top surfaces $\pm(201)$ and side surfaces $\pm(10\bar{1})$ and their growth direction is [010]. Each PbO_2 nanobelt is found to have a large polyhedral Pb tip at one of its ends, suggesting the growth is dominated by a vapor–liquid–solid mechanism. Electron beam irradiation of the PbO_2 nanobelts results in the phase transformation from PbO_2 to PbO and finally to Pb. © *2002 American Institute of Physics.* [DOI: 10.1063/1.1432749]

In the past decade, one-dimensional nanostructures, such as nanotubes and nanowires, have attracted extraordinary attention for their novel physical properties and potential applications in constructing nanoscale electronic and optoelectronic devices.[1–4] Up to now, a variety of one-dimensional nanostructures with different morphologies and compositions has been successfully fabricated by various techniques including arc discharge,[5] laser ablation,[6,7] chemical vapor deposition,[8] thermal evaporation,[9,10] and soft chemistry.[11] While a major part of work has been focused on carbon nanotubes[5,8] and semiconductor nanowires such as carbide,[12] nitride,[13] compound semiconductors,[7,14] and element semiconductors,[6,9] only a few studies on oxides including nanowires of GeO_2,[15] MgO,[16] Ga_2O_3,[17] and ZnO[18] were reported. Recently, we reported the synthesis of belt-like one-dimensional nanostructures for semiconducting oxides of zinc, tin, indium, cadmium, and gallium by simply evaporating desired commercial metal oxides powders at high temperature.[19–21] These semiconducting oxide nanobelts have a rectangle cross section that is distinctive from the previously reported cylindrical cross-section nanotubes and nanowires, which might make the belts an ideal system for fully understanding dimensionally confined transport phenomena in nanometer scale. It was suggested that such kinds of nanobelt structures could also be formed in other oxide systems.[19] In this study we will present a fabrication and structural characterization of PbO_2 nanobelts synthesized by elevated evaporation of PbO powders.

The synthesis was carried out in a horizontal tube furnace. Commercial (Alfa Asar) PbO powders with a purity of 99.99% (metal basis) were used as source material filled in an alumina crucible. The crucible together with the PbO powders was then placed at the center of an alumina tube that was inserted in the tube furnace, where the temperature, pressure, and evaporation time were controlled. Several alumina strip plates (60×10 mm^2) were placed downstream one-by-one inside the alumina tube to act as substrates for collecting growth products. After evacuating the alumina tube to $\sim2\times10^{-3}$ Torr, the elevated evaporation was conducted at 950 °C for 1 h under a pressure of 300 Torr and an Ar carrying gas with flow rate of 50 standard cubic centimeters per minutes (sccm). The products deposited on the surface of the alumina strip substrates were characterized by scanning electron microscopy (SEM), transmission electron microscopy (TEM), and energy dispersive x-ray spectroscopy (EDS).

The as-synthesized products display a dark gray color that is distinctive from the yellow color PbO source powders. SEM observations reveal that the products consist of a large quantity of belt-like nanostructures and faceted particles with diameters in the range of 0.1–2 μm [Fig. 1(a)]. Chemical analysis by EDS indicates that the belt-like nanostructures are PbO_2 and the particles are metal Pb covered with a thin oxide layer. Figures 1(b)–1(d) are bright-field TEM images showing morphology of the belt-like nanostructures, where twist [Fig. 1(c)], especially the ''M'' shaped twist [Fig. 1(d)], a characteristic feature of belt, is clearly seen. The PbO_2 nanobelts are several tens to several hundreds of micrometers in their length. Each nanobelt has a uniform width over its entire length, and the typical width of the belts is in the range of 50–300 nm. The thickness of the belt varies with its width, and typically in the range of 10–30 nm, as estimated by TEM observations. The width-to-thickness ratio of the belts is about 5–10. It is noted that each nanobelt is connected with a Pb particle at its growth front [Figs. 1(b) and 1(c)], implying that the Pb tip likely acts as a catalyst in growth of the nanobelt. The diameter of the Pb tips is several times bigger than the width of connecting nanobelts. The Pb tips have the faceted geometrical shape of an octagonal projection [Figs. 1(b) and 1(c)], which indicates that Pb tips are crystalline and likely adopt the shape of truncated octahedron enclosed by {100} and {111} crystal planes because of lower surface energies.

PbO_2 can form α and β two possible crystal structures of orthorhombic and tetragonal lattice, respectively.[22,23] Electron diffraction [Fig. 2(c)] analysis and high resolution TEM imaging [Fig. 1(b)] indicate that the as-synthesized PbO_2 nanobelt [Fig. 2(a)] is single crystalline without dislocation and has a tetragonal structure ($P4/mnm$, $a=4.961$ Å and

a)Electronic mail: zhongwang@mse.gatech.edu

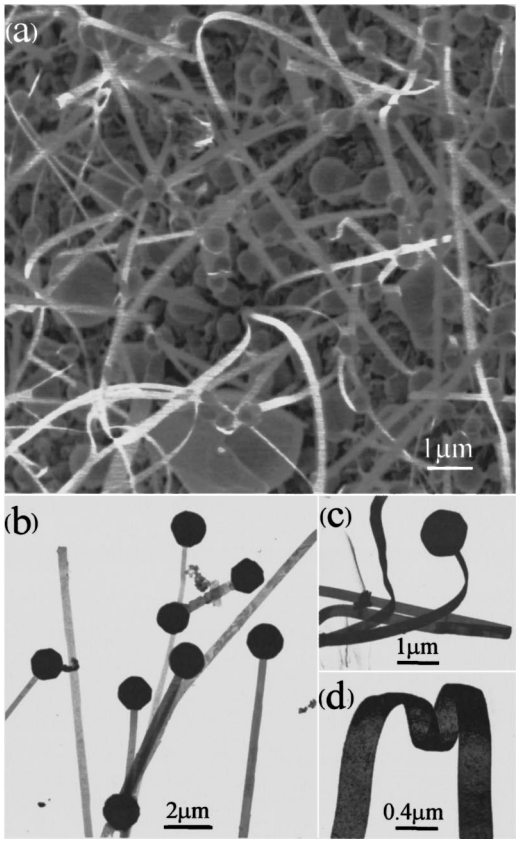

FIG. 1. (a) SEM image of the as-synthesized PbO_2 nanobelts and Pb particles; (b)–(d) are bright-field TEM images of the PbO_2 nanobelts, showing that each nanobelt has a Pb tip, and (c)–(d) display the twist feature of the nanobelt.

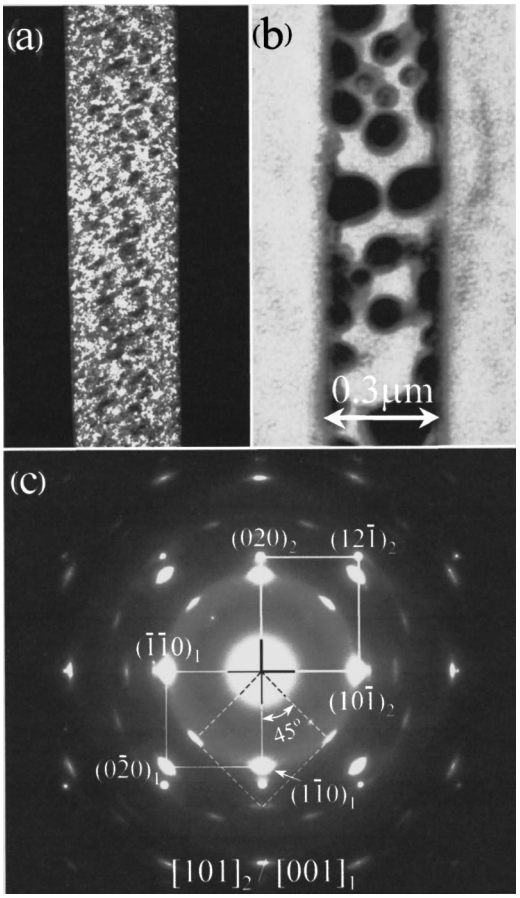

FIG. 3. (a) Dark-field TEM image of a PbO_2 nanobelt post to electron beam irradiation, where the mottled contrast indicates occurrence of precipitation. (b) Bright-field TEM image of a PbO_2 nanobelt after undergoing a long time irradiation, in which PbO_2 has decomposed into metal Pb; (c) electron diffraction pattern of the nanobelt shown in (a), displaying the phase transformation from PbO_2 to PbO.

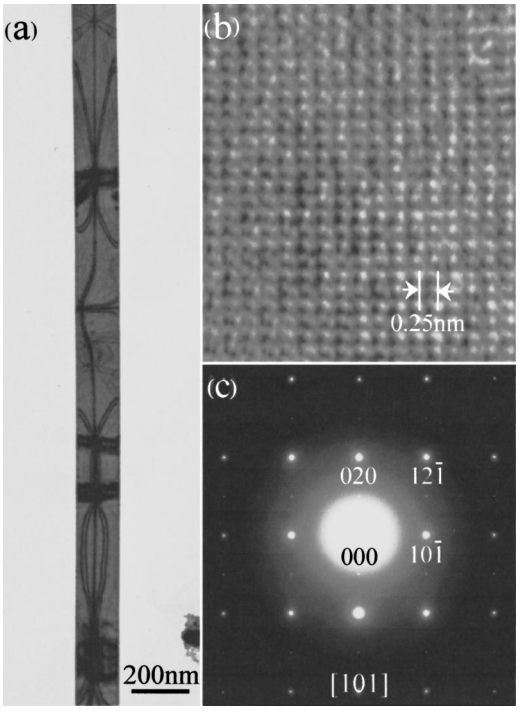

FIG. 2. Bright-field TEM image of a PbO_2 nanobelts (a), and the corresponding HRTEM image (b), and electron diffraction pattern (c).

$c=3.385$ Å),[23] i.e., β-PbO_2 nanobelts are formed. The contrast pattern over the nanobelt shown in Fig. 2(a) is bending contour. The nanobelt is enclosed by top surfaces $\pm(201)$ and side surfaces $\pm(101)$. The growth direction of the nanobelt is parallel to [010] with growth front (010).

The growth characteristics of the PbO_2 nanobelts is quite different from that of ZnO, SnO_2, In_2O_3, CdO, and Ga_2O_3 nanobelts described in Refs. 19–21, in which no particle was found at the growth fronts of the nanobelts. This implies that a different growth mechanism be employed by the PbO_2 nanobelts. The growth of the former five oxide nanobelts[19–21] is suggested to be governed by a vapor-liquid process.[24] As to the PbO_2 nanobelts described here, the growth is likely to be controlled by the vapor–liquid–solid process[25] which was suggested for the nanowires grown by a catalytic-assisted technique,[6,7,14] in which a metal particle is definitely located at the growth front of the wire and acts as the catalytic active site.

The PbO_2 nanobelts are very sensitive to electron beam irradiation under high vacuum condition in electron microscope. Figure 3(a) is a dark-field TEM image of a PbO_2 nanobelt, which is taken after the nanobelt has been illuminated by electron beam for a certain time. A mottled contrast is displayed over the nanobelt [Fig. 3(a)], implying occurrence of some precipitation under the electron beam irradia-

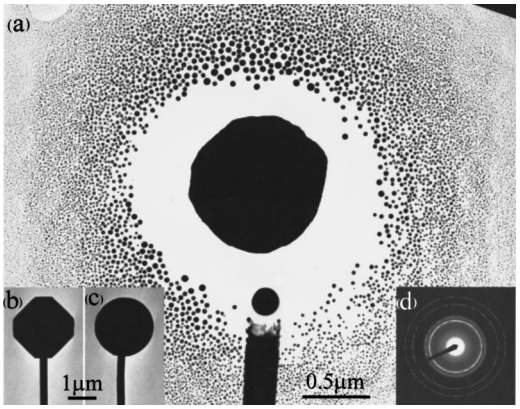

FIG. 4. (a) Bright-field TEM image of a Pb tip strongly irradiated by a converging electron beam, showing the producing of Pb nanocrystals; (b) original morphology of the crystalline Pb tip; (c) same Pb tip post to mild electron beam irradiation, displaying a molten shape; (d) selected area electron diffraction pattern of the Pb nanocrystals given in (a).

tion. Shown in Fig. 3(c) is a corresponding electron diffraction pattern, in which two sets of patterns can be identified. One is from tetragonal PbO_2 that is original phase as synthesized. The thick line frame marked in the pattern [Fig. 3(c)] represents basic unit of the diffraction pattern corresponding the tetragonal PbO_2 and its reflections are indexed with a subscript ''2.'' The other pattern is determined to be red tetragonal PbO ($P4/nmm$, $a=3.961$ Å and $c=5.011$ Å),[26] as marked by a thin line frame. The corresponding reflections are indexed with a subscript ''1.'' This indicates that the original PbO_2 phase transforms into a PbO phase by electron beam irradiation under a high vacuum condition due to pumping off the O_2 decomposed from the PbO_2. The dominant orientation relationship between the PbO_2 and the PbO is determined to be $(010)_2\|(100)_1$ and $[101]_2\|[001]_1$. Another preferable orientation of the PbO phase precipitation is that as indicated by a dotted line frame, which rotates a 45° relative to the former case. Further illuminating the nanobelt, the PbO will completely decompose into metal Pb, as shown in Fig. 3(b).

Another interested phenomenon is that the polyhedral Pb tip [Fig. 4(b)] changes into a spherical shape [Fig. 4(c)] under electron beam irradiating, indicating that a crystalline Pb tip can be melted by the irradiation due to its lower melting point. If we suddenly converge the electron beam onto the melting Pb tip, a fraction of the molten Pb will erupt off, because of thermal and charge effects from electron beam irradiation, to produce a monolayer of nanoparticles homogeneously distributed onto the carbon supporting film around the Pb tip. Select area electron diffraction [Fig. 4(d)] indicates that the nanoparticles are Pb nanocrystals. The size of the Pb nanocrystals varies from 5–50 nm depending on the distance away from the Pb tip. The farther the distance is, the finer the Pb nanocrystals are. The eruption induced by electron beam irradiation might be an interesting approach for producing nanocrystals of the metals with lower melting points.

In conclusion, tetragonal structured PbO_2 nanobelts have been synthesized by elevated evaporation of commercial PbO powders. The PbO_2 nanobelts have been determined to be enclosed by top surfaces $\pm(201)$ and side surfaces $\pm(101)$. The growth direction of the nanobelts is parallel to [010], along with a typical length of several hundred micrometers, width of 50–300 nm, and width-to-thickness ratio of 5–10. Each PbO_2 nanobelt is found to have a large polyhedral Pb tip at its growth front, suggesting that the growth of the PbO_2 nanobelts is likely controlled by a vapor-liquid-solid mechanism. The PbO_2 nanobelts and the crystalline Pb tips are very sensitive to electron beam irradiation, resulting in the phase transformation from PbO_2 to PbO, melting of the Pb tips, and formation of Pb nanocrystals under a high vacuum condition.

The authors thank the U.S. NSF for financial support from Grant Nos. DMR-9733160, the Georgia Tech Electron Microscopy Center for providing the research facilities.

[1] A. P. Alivisatos, Science **271**, 993 (1996).
[2] B. I. Yakobson and R. E. Smalley, Am. Sci. **85**, 324 (1997).
[3] J. Hu, T. W. Odom, and C. M. Lieber, Acc. Chem. Res. **32**, 435 (1999).
[4] C. Dekker, Phys. Today **52**, 22 (1999).
[5] S. Iijima, Nature (London) **354**, 56 (1991).
[6] A. M. Morales and C. M. Lieber, Science **279**, 208 (1998).
[7] X. F. Duan and C. M. Lieber, Adv. Mater. **12**, 298 (2000).
[8] Z. W. Pan, S. S. Xie, B. H. Chang, C. Y. Wang, L. Lu, W. Liu, W. Y. Zhou, W. Z. Li, and L. X. Qian, Nature (London) **394**, 631 (1998).
[9] S. T. Lee, N. Wang, Y. F. Zjang, and Y. H. Tang, Mater. Res. Bull. **24**, 36 (1999).
[10] Z. W. Pan, Z. R. Dai, L. Xu, S. T. Lee, and Z. L. Wang, J. Phys. Chem. B **105**, 2507 (2001).
[11] T. J. Trentler, K. M. Hickman, S. C. Goel, A. M. Viano, P. C. Gibbons, and W. E. Buhro, Science **270**, 1791 (1995).
[12] H. J. Dai, E. W. Wong, Y. Z. Lu, S. S. Fan, and C. M. Lieber, Nature (London) **375**, 769 (1995).
[13] W. Q. Han, S. S. Fan, Q. Q. Li, and Y. D. Hu, Science **277**, 1287 (1997).
[14] X. F. Duan, Y. Huang, Y. Cui, J. Wang, and C. M. Lieber, Nature (London) **409**, 66 (2001).
[15] Z. G. Bai, D. P. Yu, H. Z. Zhang, Y. Ding, X. Z. Gai, Q. L. Hang, G. C. Xiong, and S. Q. Feng, Chem. Phys. Lett. **303**, 311 (1999).
[16] P. Yang and C. M. Lieber, J. Mater. Res. **12**, 2981 (1997).
[17] Y. C. Choi, W. S. Kim, Y. S. Park, S. M. Lee, D. J. Bae, Y. H. Lee, G. S. Park, W. B. Choi, N. S. Lee, and J. M. Kim, Adv. Mater. **12**, 746 (2000).
[18] M. H. Huang, Y. Wu, H. Feick, N. Tran, E. Weber, and P. Yang, Adv. Mater. **13**, 113 (2001).
[19] Z. W. Pan, Z. R. Dai, and Z. L. Wang, Science **291**, 1947 (2001).
[20] Z. R. Dai, Z. W. Pan, and Z. L. Wang, Solid State Commun. **118**, 351 (2001).
[21] Z. R. Dai, Z. W. Pan, and Z. L. Wang, J. Phys. Chem. B (in press).
[22] J. E. Taggart, E. E. Foord, A. Rosenzweig, and T. Hanson, Can. Mineral. **26**, 905 (1988).
[23] H. Harada, J. Appl. Crystallogr. **14**, 141 (1981).
[24] S. S. Brenner and G. W. Sears, Acta Metall. **4**, 268 (1956).
[25] R. S. Wagner and W. C. Ellis, Appl. Phys. Lett. **4**, 89 (1964).
[26] J. Leciejewicz, Acta Crystallogr. **14**, 1304 (1961).